Pressure-tuned Frustration of Magnetic Coupling in Elemental Europium

Shu-Ting Pi, Sergey Y. Savrasov, and Warren E. Pickett*
Department of Physics, University of California Davis, Davis, California 95616 USA

(Received 30 May 2018; revised manuscript received 26 December 2018; published 6 February 2019)

Applying linear response and the magnetic force theorem in correlated density functional theory, the intersublattice exchange constants of antiferromagnetic Eu are calculated and found to vanish near the pressure of $P_c = 82$ GPa, just where magnetic order is observed experimentally to be lost. The Eu $4f^7$ moment remains unchanged at high pressure, again in agreement with spectroscopic measurements, leaving the picture of perfect frustration of interatomic Ruderman-Kittel-Kasuya-Yoshida couplings in a broad metallic background, leaving a state of electrons strongly exchange coupled to arbitrarily oriented, possibly quasistatic local moments. This strongly frustrated state gives way to superconductivity at $T_c = 1.7$ K, observed experimentally. These phenomena, and free energy considerations related to correlations, suggest an unusual phase of matter that is discussed within the scenarios of the Doniach Kondo lattice phase diagram, the metallic spin glass class, and itinerant spin liquid or spin gas systems.

DOI: 10.1103/PhysRevLett.122.057201

The behavior of local moments and their ordering as some external parameter (volume, electron density, magnetic field) varies lies at the root of several paradigmatic phenomena, viz. the Kondo effect, heavy fermion superconductivity, spin liquid, and spin glass phases. The $4f$ shell in lanthanides (Ln) has provided a unique platform for the study of several of these issues. Ce and Yb compounds, with their $4f$ level near the Fermi energy, show $4f$-conduction electron coupling that can be tuned across the Doniach critical point from antiferromagnet (AFM) to Kondo lattice at ambient pressure. Reduction in volume is needed to drive other lanthanides into exotic phases.

Experimentally, a study by Jackson *et al.* [1] of six Ln metals with pressure tuned in the 5–12 GPa range indicated a linear decrease in the magnetic ordering temperature T_m roughly in proportion to the de Gennes factor of the $4f$ ion. However, higher pressures bring more complex behavior due to structural transitions and band structure changes. In the lanthanides (Ln) Tb, Dy, and Nd, T_m varies as much as 150 K through pressure ranges up to 1.5 mbar [2–4], often nonmonotonically. In Eu, however, after nonmonotonic behavior in $T_m(P)$ due to structural transitions [5,6], in the *Pnma* structure that exists in a range around 80 GPa, T_m falls to 11 K at $P_c = 82$ GPa whereupon magnetic order is replaced with superconductivity (SC) up to 3 K [7].

Advances in modeling exchange coupling in Ln metal [8–11] have dealt with *ordering*. This first order disappearance of order represents an *avoidance* of the antiferromagnetic (AFM) quantum critical point that is actively studied in weak AFMs [12]. This paramagnetic (PM) phase, with its SC ground state in the midst of disordered spin, may provide a platform for learning more about Ln magnetic interactions, and perhaps more general issues about neighboring phases near a QCP, possibly including a spin liquid or spin gas phase coexisting with SC.

This behavior can be compared with that of Yb. Under pressure, Yb undergoes a valence transition [13–16] from divalent f^{14} to somewhere near trivalent f^{13} through a continuous evolution through intermediate valence and emergence of a local moment, a crossover that has been simulated successfully by dynamical mean field calculations [16] up to 40 GPa. Recently Song and Schilling have reported [17] that Yb, notwithstanding its f^{13} local moments, becomes superconducting in the 1.4–4.5 K range at 80 GPa and above. This behavior has parallels with, but distinctions to, that of Eu, to which we return to in the discussion.

The PM phase above P_c is unusual in having large spins on a dense periodic lattice interacting via RKKY Heisenberg exchange (the spins are isotropic) yet they do not order, a signature of a type of frustration that is not apparent. Following the classification of Sachdev and Read [18], we refer to this as the metallic quantum paramagnet (MQPM) phase. Beyond the question of (dis)ordering, there is the perplexing issue of superconductivity in a metal with disordered strong local moments. A simple scenario would be that Eu would be driven through a valence transition to the nonmagnetic f^6 $J = 0$ configuration, in which case there is no magnetic impediment to superconducting pairing, viz. the isovalent rare earth metal Y becomes an impressive superconductor under pressure, with T_c up to 17 K [19]. We find that Eu, unlike Yb, is not near a change in valence up to 100 GPa or more.

While early studies suggested a valence transition below 80 GPa [20], more recent x-ray absorption confirm that Eu retains its f^7 moment even in the SC phase above 82 GPa

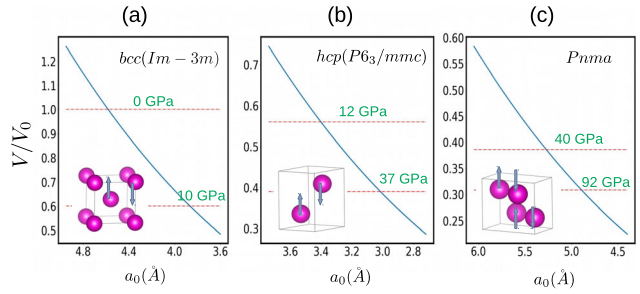

FIG. 1. The relative volume V/V_0 ratio as a function of the a lattice constant (a) bcc, (b) hcp, and (c) $Pnma$. The lattice structures were obtained from experiments. Red dashed lines indicate the V/V_0 ratio of pressures where the structures are confirmed stable in experiments, as given by Bi *et al.* [5].

[17,21] in agreement with our calculations. The SC phase is then of an exotic type in which pairing occurs within a dense lattice of large but disordered and uncompensated moments. These questions have led us to perform systematic calculations of the electronic structure and magnetic coupling of Eu at pressures up to the 100 GPa range.

Like all Ln metals, Eu displays structural transformations with increasing pressure. Structural information is provided in the Supplemental Material (SM [22]). The volume decrease V/V_0 ratio (V_0 is the ambient volume) and the regions of stability of the three phases [5] are shown with the magnetic structures in Fig. 1. The evidence is that Eu displays AFM order from ambient to $P_c = 82$ GPa. At P_c, magnetic order vanishes and superconductivity emerges with critical temperature $T_c = 1.7$ K, increasing with pressure up to 2.8 K at 142 GPa [7]. As recently reported [6] and as we confirm from our calculations, the large moment on Eu persists (the f^7 moment in Gd is calculated [23] to persist to 500 GPa), making the interplay between large but disordered moments and SC, and its dependence on pressure, unresolved issues.

Our density functional theory (DFT) calculations employ the full potential linearized-muffin-tin-orbital method (LMTO) [24]. The local spin density approximation (LSDA) with Hubbard U correction (LSDA + U) is applied to the localized $4f$ shell orbitals of Eu, using the localized limit functional implemented in the LMTO package in rotationally invariant fashion [25,26]. A reasonable value is $U = 6$–7 eV at ambient pressure [27]; we have used $U = 7$ eV and $J = 1$ eV at zero pressure, and at high pressure we investigate smaller values of U. We use LSDA + U rather than LDA + U because the spin-density mediated intra-atomic $f - d$ Hund's coupling that polarizes the conduction electrons is important to include and assess. See Supplemental Material SM [22] for additional information.

Interatomic RKKY exchange constants are known to extend out to dozens of neighboring shells in Eu [27,28]. Instead we focus on the AFM sublattice exchange constants, which are linear combinations of interatomic exchange constants out to arbitrary distance. An effective and efficient method is to use linear response theory and the magnetic force theorem [29]. Consider the electronic Kohn-Sham Hamiltonian $H_{\rm KS} = T + V_0 + V_{\rm sp}$, where T is kinetic energy, V_0 is the spin-independent potential, and $V_{\rm sp}$ is the spin-dependent potential including the contribution from U. We write $V_{\rm sp} = \vec{\sigma} \cdot \mathbf{B}$, $\mathbf{B} = [v_{xc,\uparrow}(r) - v_{xc,\downarrow}(r)]\hat{B}$, where $\vec{\sigma}$ is the electron spin vector of Pauli matrices. $\mathbf{B}$ appears as an effective Zeeman field arising from the spin-dependent exchange-correlation potential v_{xc}.

If one rotates the moment on AFM sublattices τ, τ' in unit cells $\mathbf{R}$, $\mathbf{R}'$ by infinitesimal angles $\delta\theta_{\tau R}$, $\delta\theta_{\tau' R'}$, respectively, the second order energy difference is related to the exchange constants by

$$J^{\alpha\beta}_{\tau R \tau' R'} = \frac{\delta^2 E}{\partial\theta^{\alpha}_{\tau R}\partial\theta^{\beta}_{\tau' R'}} = \sum_q J^{\alpha\beta}_{\tau\tau'}(q) e^{iq(R-R')}, \tag{1}$$

$$J^{\alpha\beta}_{\tau\tau'}(q) = \sum_{kjj'} B^{\tau\alpha}_{kj;k+q.j'} B^{\tau'\beta *}_{kj;k+q.j'} \frac{f_{kj} - f_{k+qj'}}{\epsilon_{kj} - \epsilon_{k+qj'}}, \tag{2}$$

$$B^{\tau\alpha}_{kj;k+q.j'} = \langle kj|[\sigma \times \mathbf{B}_\tau]_\alpha|k + qj'\rangle. \tag{3}$$

Here j, j' are band indices, α, β are Cartesian coordinates, k, q are wave vectors, f_{kj} is the Fermi function, ϵ_{kj} and $|kj\rangle$ are the LSDA + U energies and eigenstates. This method has been confirmed to work well in several transition metal oxides and rare earth compounds. A version extended to systems with strong spin-orbit coupling and multipolar exchange interactions was also proposed and applied successfully [8,9].

The initial questions to address are the $4f$ occupation and the position of the $4f$ levels with respect to the Fermi energy E_F. Technical details are provided in the SM. For all structures and pressures studied, the full $S = \frac{7}{2}$ $4f$ contribution persisted, with a conduction band ($5d$) contribution of 0.1–0.2 μ_B when spins were aligned. The $4f$ bands are centered near -5 eV, with the main change with pressure being that the $4f$ band "width" increases, primarily a crystal field increase rather than a hopping amplitude increase. For comparison, the $4f^7$ configuration of Gd has been calculated to remain stable to 500 GPa and above [23]. To indicate the magnitude of the exchange constants and provide connection with future experiments, the spin-wave spectrum for the ambient pressure bcc phase was calculated and is provided in the SM.

Magnetic coupling of the Ln metals in general and Eu in particular, with their nonoverlapping local moments within an itinerant electron sea, is due to the conduction electron mediated RKKY exchange mechanism described above. Throughout the pressure range studied, and in particular in the regime where magnetic order vanishes, the Fermi surface is large and multisheeted but evolving, as pictured in Fig. 2. Large sheets are separating in the vicinity of P_c, but this change in Fermi surface topology does not lead to

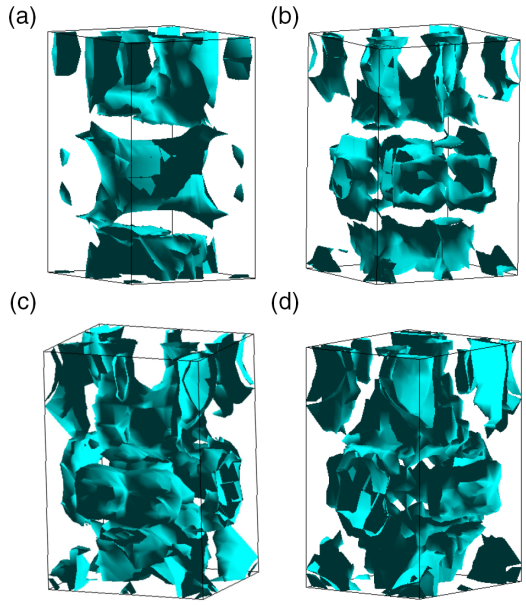

FIG. 2. The Fermi surfaces of Eu at the relative volumes (with respect to that at 75 GPa) of +6%, 0, −4%, and −10%. At all volumes the surfaces are large and multisheeted, varying through changes in topology with the only effect being the decrease in exchange constants and hence the ordering temperature, which vanishes around 82 GPa.

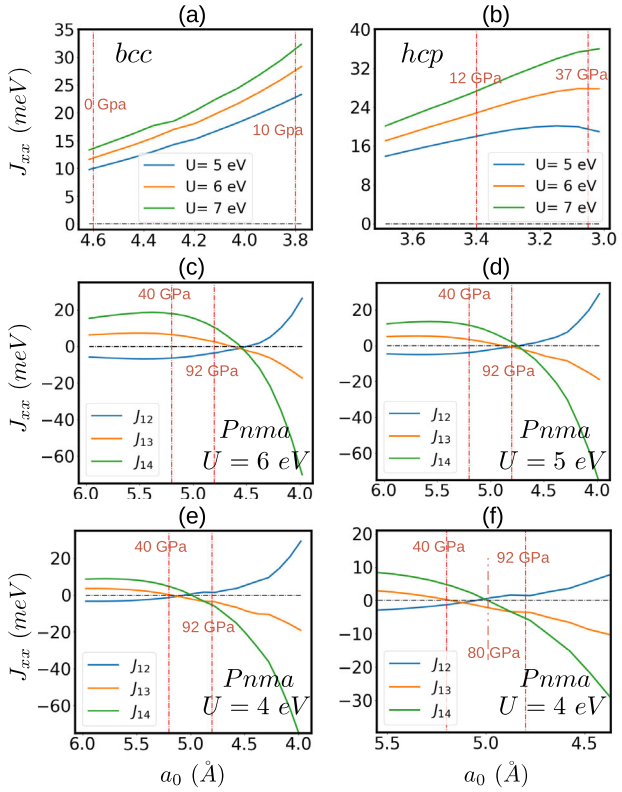

FIG. 3. The exchange constants $J_{\tau\tau'}(q=0)$ for various pressures, as labeled. Panels (a) and (b) show bcc and hcp, respectively. The others are for the *Pnma* phase at higher pressure: (c) U = 6 eV, (d) U = 5 eV, (e) U = 4 eV. Panel (f) focuses more closely on the sign change region in (e), showing that the zero crossings lie close to 80 GPa. Red dashed lines represent experimental pressures at the displayed lattice constants.

significant van Hove singularities in the density of states nor to identifiable structure in J_{ij} versus pressure. While spiral magnetic order is commonly identified with nesting of sheets of Fermi surface, a stable AFM order while the Fermi surface evolves argues against any nesting origin of ordering.

Equations (2)–(4) were used to calculate the sublattice exchange constants $J_{\tau\tau'}$ based on the AFM ordered state. With two up and two down spins, symmetry reduces the number of constants to three, viz. up1-up1, up1-down1, up1-down2, denoted below by J_{12}, J_{13}, J_{14}, respectively. The RKKY expression includes momentum-conserving virtual excitations, with those near the Fermi level having larger weight. In the $q \to 0$ limit, inter-sub-lattice exchange constants contain distinct intraband and interband terms (for general q there is no distinction). The energy denominator makes exchange coupling somewhat sensitive to Fermi surface nesting, and several examples of incommensurate (often spiral) order in lanthanides have been traced back to Fermi surface calipers. The interband contribution will be continuous and more slowly varying than the intraband contribution. The calculated $J_{\tau\tau'}(q=0)$ couplings versus pressure are shown in Fig. 3 for $U = 5$, 6, 7 eV. For bcc and hcp Eu, see Figs. 3(a) and 3(b), respectively, the single sublattice coupling is FM for J_{12} and AFM in sign for the other two, and each increases monotonically in magnitude over the range of interest.

The behavior in the high pressure *Pnma* structure is different. In Figs. 4(c)–4(f) J_{12}, J_{13}, and J_{14} at $\vec{q} = 0$ are shown, with increasing pressure and for $U = 4$, 5, 6 eV. U affects primarily the magnitude, and does not change the behavior as volume is reduced. The trend with increasing pressure is for *all three sublattice couplings* to decrease in magnitude and pass through zero nearly simultaneously, signaling a collapse of the spin-wave spectrum and frustration of *sublattice coupling* rather than frustration of magnetic order. This trend is nearly independent of the value of U; the collapse occurs at somewhat lower pressure as U is decreased. U is expected to decrease under pressure from the $U = 6$–7 eV value that is realistic [27] at ambient pressure. Note that the curves in Figs. 3(c)–3(f) become unphysical beyond P_c. It is not unusual in highly frustrated magnets to encounter a range of exchange couplings for which AFM order vanishes.

Eu thus provides a contrast to the Fe pnictides where impact of magnetic interactions on the phase diagram has been actively studied. Our methods applied to Fe pnictides led to (1) effective short-range coupling, and (2) AFM order that vanishes due to first neighbor (J_1) and second neighbor (J_2) coupling as $J_1/2J_2$ approaches unity [30,31]. Such a $J_1 - J_2$ model near frustration, with spins damped by

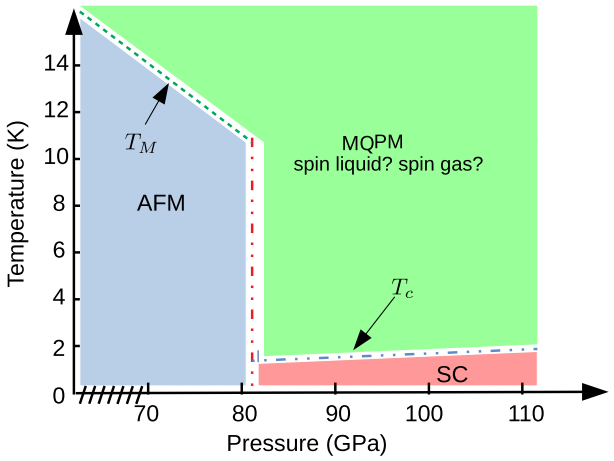

FIG. 4. Schematic depiction of the experimental phase diagram of Eu under pressure, showing the first order transition at $P_c = 82$ GPa. Phases are these: MQPM, metallic quantum paramagnetic; AFM, antiferromagnetic; SC, superconducting.

conduction electrons, was proposed by Wu *et al.* [32,33] to account for the quantum critical point versus isoelectronic As → P doping in $BaFe_2As_2$. Recently Sapkota *et al.* [34] reported near-perfect $J_1 - J_2$ frustration in an itinerant metallic system, square lattice $CaCo_{1.86}As_2$ tuned (naturally) by Co vacancies. Frustration in Eu is in a stoichiometric lattice with local moments and RKKY interactions, so the mechanism of frustration—volume evolution of many exchange constants—is distinct.

Discussion.—Both experiment and our calculations concur that Eu retains its f^7 local moment without valence change [6], and magnetic coupling vanishes at P_c. Evidently the evolution of the electronic structure plays a critical role by inducing a AFM-MQPM transition. That the three independent couplings vanish together at $P \approx P_c = 82$ GPa suggests that the Kondo coupling between spin and conduction electrons dominates RKKY coupling [35] and has decreased dramatically with pressure. We have calculated the hybridization function [36] and determined that this is not the case.

A schematic phase diagram based on experimental data is presented in Fig. 4. Magnetic order decreasing to 11 K vanishes at P_c, and superconducting electronic order emerges as the ground state of this MQPM. This ground state presents a potentially new phase: a superconducting condensate in the midst of large disordered moments (not compensated by Kondo coupling) below $T_c = 1.7$ K. The character of the transition from AFM order to an MQPM phase at P_c seems intimately related to the question of magnetic correlations in the MQPM phase. In the free energy $F(P,T) = E_{\mathrm{DFT}}[V(P)] + PV_{\mathrm{DFT}}(P) + E_m(P,T) - TS_m(P,T)$ the first two quantities are available from DFT calculations and are linear in P and T independent at low T since (1) no structural change occurs [5], and (2) the magnetic moments remain, only the magnetic order vanishes [6]. The electronic entropy $(\pi^2/3)k_BTN(E_F) \sim (\pi^2/3)k_BT/W$, where the bandwidth is $W = \sim$2–4 eV, is orders of magnitude smaller than the magnetic terms, and has not been displayed.

The magnetic contributions, E_m and S_m from spin waves in the AFM phase, or spin disorder in the PM phase, must account for the small free energy change across the transition. The difference in entropy between ordered and uncorrelated moments at high temperature is $S^\infty = k_B \ln(2S+1) = 3k_B \ln 2$ for $S = \frac{7}{2}$. A rough (factor of two) estimate of the entropy of the ordered phase can be taken from the linear spin-wave theory expression $S_{\mathrm{AFM}} = \beta(P)T^3$; β is P dependent because it depends on the exchange couplings $\{J_{\tau\tau'}\}$. The entropy just above T_N is roughly $S^\infty/2$, a common value for AFMs. Equating these at T_N, one obtains the change across the transition as temperature is lowered for $P < P_c$

$$\Delta(TS_m(P,T)) \approx \frac{1}{2}S^\infty T\left(1 - \frac{T^3}{T_N(P)^3}\right), \tag{4}$$

which is smooth and small across the magnetic transition but becomes sizable at a somewhat lower temperature.

However, supposing uncorrelated moments for $P > P_c$, the change in entropy across P_c has the same form: the increase in entropy contributes to the loss of magnetic order above P_c, with a finite jump for $T < T_N(P_c) = 11$ K but vanishing at (P_c, T_N), giving no driving force for a first order transition *at this point* in the phase diagram.

The magnetic energy E_m of thermally excited spin waves, $E_m(P,T) = \int d\omega D(\omega,P)n(\omega/T)$ in terms of the spin-wave density of states D and the Bose occupation factor $n(\omega/T)$, is replaced above P_c with contributions depending on the degree of magnetic correlation among the disordered spins. Total lack of correlation is unrealistic, in fact, considerable short-range correlation must survive to leave only a small change in the free energy at P_c. The result: the necessary small change in free energy across P_c implies spin correlations in the MQPM phase, possible characterizations being a spin liquid [37] or spin glass [38]. YMn_2 and $CaCo_{1.86}As_2$ both are magnetic metals that have been discussed as spin liquids [34,39], but unlike Eu they are understood in terms of frustrating short-range interactions.

In closing, we comment on the unconventional electronic state in the SC phase. The scenario that has emerged is that of superconducting pairs coexisting with a spin glass or spin liquid magnetic system, presumed classical given the large value of the moments. With negligible quantum fluctuation and the temperature being low compared to other scales, one has pairing in the midst of quasistatic spins. Superconductivity in the context of spin glasses has been discussed, for example by Galitski and Larkin [40], and an example proposed by Davidov *et al.* [41]; however spin glasses are nearly always treated in the dilute impurity limit where positional disorder is a central issue, whereas

the spins in Eu are dense and periodic. Our calculated exchange splitting of the Eu d bands for ferromagnetic alignment indicates a local on site $f-d$ Hund's exchange strength near 1 eV, corresponding to a FM Kondo coupling of $K = 1.0/(\frac{7}{2} \times \frac{1}{2}) \sim 0.5$ eV. This strong coupling suggests comparable spin-disorder broadening of the conduction bands, hence washing out of the Fermi surface. Spin-disorder is normally destructive of pairing, unless the mechanism actually proceeds through, and depends on, the dynamic spin system. Such pairing, if it is responsible, lies in a different regime in Eu than for the cuprates, Fe-based superconductors, and heavy fermions, where magnetic fluctuations of small moments are intimately mixed into the conduction states. Yb at high pressure, as discussed in the introduction, presents a SC phase that may possess similarities to that of Eu.

We thank Wei-Ting Chiu, R. Kremer, R. R. P. Singh, J. Oitmaa, and J. S. Schilling for helpful communications on this project. Support from DOE NNSA Grant No. DE-NA0002908 (S. T. P.), NSF Grant No. DMR-1411336 (S. Y. S.), and NSF Grant No. DMR-1607139 (W. E. P.) are gratefully acknowledged. For computational facilities, we used the National Energy Research Scientific Computing Center (NERSC), a DOE Office of Science User Facility supported by DOE under Contract No. DE-AC02-05CH11231, as well as an in-house cluster at UC Davis.

*wepickett@ucdavis.edu

[1] D. D. Jackson, V. Malba, S. T. Weir, P. A. Baker, and Y. K. Vohra, High-pressure magnetic susceptibility experiments on the heavy lanthanides Gd, Tb, Dy, Ho, Er, and Tm, Phys. Rev. B **71**, 184416 (2005).

[2] J. Lim, G. Fabbris, D. Haskel, and J. S. Schilling, Anomalous pressure dependence of magnetic ordering temperature in Tb revealed by resistivity measurements to 141 GPa: Comparison with Gd and Dy, Phys. Rev. B **91**, 174428 (2015).

[3] J. Lim, G. Fabbris, D. Haskel, and J. S. Schilling, Magnetic ordering at anomalously high temperatures in Dy at extreme pressures, Phys. Rev. B **91**, 045116 (2015).

[4] J. Song, W. Bi, D. Haskel, and J. S. Schilling, Evidence for strong enhancement of the magnetic ordering temperature of trivalent Nd metal under extreme pressure, Phys. Rev. B **95**, 205138 (2017).

[5] W. Bi, Y. Meng, R. S. Kumar, A. L. Cornelius, W. W. Tipton, R. G. Hennig, Y. Zhang, C. Chen, and J. S. Schilling, Pressure-induced structural transitions in europium to 92 GPa, Phys. Rev. B **83**, 104106 (2011).

[6] W. Bi *et al.*, Magnetism of europium under extreme pressures, Phys. Rev. B **93**, 184424 (2016).

[7] M. Debessai, T. Matsuoka, J. J. Hamlin, J. S. Schilling, and K. Shimizu, Pressure-Induced Superconducting State of Europium Metal at Low Temperatures, Phys. Rev. Lett. **102**, 197002 (2009).

[8] S.-T. Pi, R. Nanguneri, and S. Savrasov, Calculation of Multipolar Exchange Interactions in Spin-Orbital Coupled Systems, Phys. Rev. Lett. **112**, 077203 (2014).

[9] S.-T. Pi, R. Nanguneri, and S. Savrasov, Anisotropic multipolar exchange interactions in systems with strong spin-orbit coupling, Phys. Rev. B **90**, 045148 (2014).

[10] I. L. M. Locht *et al.*, Standard model of the rare earths analyzed from the Hubbard I approximation, Phys. Rev. B **94**, 085137 (2016).

[11] E. Mendive-Tapia and J. B. Staunton, Theory of Magnetic Ordering in the Heavy Rare Earths: *Ab Initio* Electronic Origin of Pair- and Four-Spin Interactions, Phys. Rev. Lett. **118**, 197202 (2017).

[12] G. Knebel, D. Aoki, C. Braithwaite, B. Salce, and J. Flouquet, Coexistence of antiferromagnetism and superconductivity in $CeRhIn_5$ under high pressure and magnetic field, Phys. Rev. B **74**, 020501(R) (2006).

[13] K. Syassen, G. Wortmann, J. Feldhaus, K. H. Frank, and G. Kaindl, Mean valence of Yb metal in the pressure range 0 to 340 kbar, Phys. Rev. B **26**, 4745 (1982).

[14] A. Fuse, G. Nakamoto, M. Kurisu, N. Ishimatsu, and H. Tanida, The valence state of Yb metal under high pressure determined by XANES measurement up to 34.6 GPa, J. Alloys Compd. **376**, 34 (2004).

[15] C. Dallera *et al.*, Understanding mixed valent materials: Effects of dynamical core-hole screening in high-pressure x-ray spectroscopy, Phys. Rev. B **74**, 081101(R) (2006).

[16] E. R. Ylvisaker, J. Kuneš, A. K. McMahan, and W. E. Pickett, Charge Fluctuations and the Valence Transition in Yb under Pressure, Phys. Rev. Lett. **102**, 246401 (2009).

[17] J. Song and J. S. Schilling, Pressure-Induced Superconductivity in Elemental Ytterbium Metal, Phys. Rev. Lett. **121**, 037004 (2018).

[18] S. Sachdev and N. Read, Metallic spin glasses, J. Phys. Condens. Matter **8**, 9723 (1996).

[19] J. J. Hamlin, V. G. Tissen, and J. S. Schilling, Superconductivity at 17 K in yttrium metal under nearly hydrostatic pressures up to 89 GPa, Phys. Rev. B **73**, 094522 (2006).

[20] J. Röhler, The valence of Eu under high pressure, Physica (Amsterdam) **144B+C**, 27 (1986).

[21] W. Bi *et al.*, Synchrotron x-ray spectroscopy studies of valence and magnetic state in europium metal to extreme pressures, Phys. Rev. B **85**, 205134 (2012).

[22] See Supplemental Material at http://link.aps.org/supplemental/10.1103/PhysRevLett.122.057201 for structural information and additional computational results.

[23] Z. P. Yin and W. E. Pickett, Stability of the Gd magnetic moment to the 500 GPa regime, Phys. Rev. B **74**, 205106 (2006).

[24] S. Yu. Savrasov and D. Yu. Savrasov, Full-potential linear-muffin-tin-orbital method for calculating total energies and forces, Phys. Rev. B **46**, 12181 (1992).

[25] S. L. Dudarev, G. A. Botton, S. Y. Savrasov, C. J. Humphreys, and A. P. Sutton, Electron-energy-loss spectra and the structural stability of nickel oxide: An LSDA + U study, Phys. Rev. B **57**, 1505 (1998).

[26] See E. R. Ylvisaker, K. Koepernik, and W. E. Pickett, Anisotropy and magnetism in the LSDA + U method, Phys. Rev. B **79**, 035103 (2009), for a description of and references to L(S)DA + U functionals.

[27] J. Kuneš and R. Laskowski, Magnetic ground state and Fermi surface of bcc Eu, Phys. Rev. B **70**, 174415 (2004).
[28] I. Turek, J. Kudrnovský, M. Diviš, P. Franek, G. Bihlmayer, and S. Blügel, First-principles study of the electronic structure and exchange interactions in bcc europium, Phys. Rev. B **68**, 224431 (2003).
[29] A. I. Liechtenstein, M. I. Katsnelson, V. P. Antropov, and V. A. Gubanov, Local spin density functional approach to the theory of exchange interactions in ferromagnetic metals and alloys, J. Magn. Magn. Mater. **67**, 65 (1987).
[30] Z. P. Yin, S. Lebegue, M. J. Han, B. P. Neal, S. Y. Savrasov, and W. E. Pickett, Electron-Hole Symmetry and Magnetic Coupling in Antiferromagnetic LaFeAsO, Phys. Rev. Lett. **101**, 047001 (2008).
[31] M. J. Han, Q. Yin, W. E. Pickett, and S. Y. Savrasov, Anisotropy, Itineracy, and Magnetic Frustration in High-T_c Iron Pnictides, Phys. Rev. Lett. **102**, 107003 (2009).
[32] Q. Si and E. Abrahams, Strong Correlations and Magnetic Frustration in the High T_c Iron Pnictides, Phys. Rev. Lett. **101**, 076401 (2008).
[33] J. D. Wu, Q. M. Si, and E. Abrahams, Magnetic and Ising quantum phase transitions in a model for isoelectronically tuned iron pnictides, Phys. Rev. B **93**, 104515 (2016).
[34] A. Sapkota *et al.*, Effective One-Dimensional Coupling in the Highly Frustrated Square-Lattice Itinerant Magnet $CaCo_{2-y}As_2$, Phys. Rev. Lett. **119**, 147201 (2017).
[35] L. Isaev, K. Aoyama, I. Paul, and I. Vekhter, Orbital Order and Hund's Rule Frustration in Kondo Lattices, Phys. Rev. Lett. **111**, 157202 (2013).
[36] M. J. Han, X. Wan, and S. Y. Savrasov, Competition between Kondo and RKKY exchange couplings in $Pu_{1-x}Am_x$ alloys: Density functional theory with static Hartree-Fock and dynamic Hubbard-I approximations, Phys. Rev. B **78**, 060401(R) (2008).
[37] L. Savary and L. Balents, Quantum spin liquids, Rep. Prog. Phys. **80**, 016502 (2017).
[38] J. A. Mydosh, Spin glasses: Redux: An updated experimental/materials survey, Rep. Prog. Phys. **78**, 052501 (2015).
[39] M. Shiga and H. Nakamura, Spin fluctuations in Itinerant frustrated systems, in *Itinerant Electron Systems: Fluctuation Effects*, NATO Science Series Vol. 55, edited by D. Wagner, W. Brauneck, and A. Solontsov (ASHT) (Springer, Dordrecht, Netherlands, 1998), pp. 1–13.
[40] V. M. Galitski and A. I. Larkin, Spin glass versus superconductivity, Phys. Rev. B **66**, 064526 (2002).
[41] D. Davidov, J. A. Mydosh, G. J. Nieuwenhuys, and K. Baberschke, Coexistence of superconductivity and spin glass magnetic freezing, J. Phys. F **7**, L47 (1977).